

Received January 23, 2018, accepted March 21, 2018, date of publication April 20, 2018, date of current version May 16, 2018.

Digital Object Identifier 10.1109/ACCESS.2018.2828788

On the Average Achievable Rate of QPSK and DQPSK OFDM Over Rapidly Fading Channels

YASHAR M. AVAL¹, SARAH KATE WILSON², (Fellow, IEEE),
AND MILICA STOJANOVIC¹, (Fellow, IEEE)

¹Northeastern University, Boston, MA 02115, USA

²Santa Clara University, Santa Clara, CA 95053, USA

Corresponding author: Yashar M. Aval (y.aval@neu.edu)

This work was supported in part by NSF under Grant CNS-1726512, in part by ONR under Grant N00014-15-1-2550, and in part by NSF under Grant 1428567.

ABSTRACT Motivated by recent experimental observations, where differentially coherent detection outperforms coherent detection on certain underwater acoustic channels, we revisit the performance of these two methods with respect to the achievable rate in orthogonal frequency-division multiplexing systems. Our comparison is based on a class of time-varying channels, where coherent quadrature phase shift keying (QPSK) detection requires channel estimation through a set of designated pilot symbols, while differentially coherent QPSK (DQPSK) enjoys an almost pilot-free detection. We show that given the cost of pilot overhead and channel estimation errors, the average rate achievable with DQPSK can be higher than that of QPSK. We use analytical results to identify channels for which this is the case, and expand the results to larger constellation sizes such as 8PSK, 16PSK, and 16QAM. In addition to acoustic channels, wireless radio channels with unusually long delay spread or high Doppler spread, such as those found in unmanned aerial systems and high-speed trains, may also benefit from using differentially coherent detection. In general, differentially coherent detection is favored in rapidly time-varying channels which require large pilot overhead and/or whose bit error rate performance is dominated by channel estimation errors. Our analysis includes the results for array receivers and soft detectors, showing that the favorable parameter range for differentially coherent detection expands significantly in both cases.

INDEX TERMS Channel capacity, information rate, bit error rate, OFDM, Rayleigh channels, underwater communication, differential phase shift keying, channel estimation.

I. INTRODUCTION

The bit error rate (BER) of quadrature phase shift keying (QPSK) and differential QPSK (DQPSK) has been extensively analyzed in the literature for both additive white Gaussian noise (AWGN) and fading channels. It is well known that coherent detection has a 3 dB gain over differentially coherent detection on Rayleigh fading channels [1]; however, this gain is contingent upon a perfectly known channel. In contrast, differentially coherent detection does not require any knowledge of the channel, and thus may perform better than QPSK due to the limitations of channel estimation accuracy and the number of pilot symbols needed to estimate the channel.

Numerous analyses have focused on the cost of channel estimation for coherent receivers operating over time-varying channels, ranging from decision-feedback equalizers (DFE)

in single-carrier mode (see e.g. [2]) and multi-carrier OFDM receivers with pilot-based channel estimation (e.g. [3], [4]), to decision-directed OFDM receivers (e.g. [5], [6]). These references, as well as other related research, show that regardless of the channel estimation method used, channel estimation becomes a challenging task in highly time-varying channels. The restrictions that it imposes should thus be considered in a meaningful performance analysis.

These facts lead to the question of whether coherent receivers can be outperformed by their differentially coherent counterparts in highly time-varying channels. Reference [7] addresses this question for single-carrier communication systems, where the effect of outdated channel estimation is shown to increase the BER of coherent QPSK receivers above that of differentially coherent receivers in the high SNR regime. It is also shown that the achievable rate follows a

similar trend with coherent receivers being outperformed for high SNR scenarios.

Reference [8] addresses the same question for OFDM communication systems by comparing the coded BER performance of a coherent receiver operating in decision-directed mode with that of a differentially coherent receiver. An interesting finding of this comparison is that in one of the scenarios, low-complexity differentially coherent detection outperforms coherent detection at higher SNRs. Although the same error correction code was used for both receivers, the coherent receiver required a training overhead of 10% compared to a negligible overhead for the differentially coherent receiver.

Another comparison is made in Reference [9], where DQPSK is shown to be capable of providing lower BER than QPSK in OFDM systems over highly time-varying channels. However, in this comparison, a pre-coding technique which dedicates half of the carriers to inter-carrier interference (ICI) reduction is used for DQPSK. Insertion of known symbols reduces the information rate by 50% which is not reflected in the BER analysis. In contrast, coherent QPSK employs ICI equalization without a significant penalty on the rate.

More recently, [10] focused on the error exponent for massive single-input multi-output (SIMO) systems operating over Ricean fading channels where the line-of-sight (LOS) component is known to the receiver. The authors reinforced the notion that with a dominant LOS, estimating the residual Rayleigh component is not worth the pilot overhead.

Finally, [11] compared the performance of QPSK and DQPSK over underwater acoustic channels through an experimental data analysis to show that DQPSK can significantly outperform QPSK both in terms of coded BER and mean squared error (MSE). The specific DQPSK receiver of [11] employed dedicated pre-processing for ICI reduction, while coherent receivers operated in decision-directed mode to track the channel from one OFDM block to the next. Although this reference does not provide a generalized comparison between QPSK and DQPSK, it carries two key conclusions. One is that DQPSK has a tendency to outperform QPSK on certain underwater acoustic channels, and the other is that there exists an effective ICI mitigation technique for OFDM receivers operating in differentially coherent mode with a negligible reduction on the information throughput.

The observations made so far motivate the need for a generalized comparison between coherent and differentially coherent receivers that is fair not only in terms of the BER, but in terms of the information throughput (bit rate) as well. Such a comparison will help in understanding why and when differentially coherent detection outperforms coherent detection.

To answer this question, we revisit the performance of QPSK and DQPSK on time-varying channels. Our present comparison differs from that of [7] in the following ways: We consider the effect of imperfect channel estimation, take the reduction of rate due to pilot overhead into account, and optimize pilot insertion strategy to ensure optimal

implementation of the coherent receiver. At the same time, our results are more general than those of [8] as we make no assumptions about a specific receiver algorithm or a specific forward error correction (FEC) code. Our work also differs from [10] as we assume that the DQPSK receiver has no additional knowledge of the channels, while the QPSK receiver depends solely on the channel estimate obtained from the pilots.

In order to provide a fair comparison between QPSK and DQPSK, we address the following two aspects. First, we take the cost of channel estimation into account. Second, we select the parameters of the QPSK receiver optimally, such that if it is outperformed by the DQPSK receiver, a suboptimal design cannot be blamed, i.e. no further improvements are possible. Our comparison is based on the average achievable bit rate, so as to fully reflect the impact of pilot overhead.¹ We focus on the framework of an OFDM system where a portion of carriers in each OFDM block are designated as pilots to assist with estimating the channel.

To ensure a proper design for the coherent receiver, we optimize the ratio of pilots, and employ a channel estimator that takes advantage of the sparseness of the channel impulse response. It is shown in [8] that this optimal division depends on the average SNR, the fading rate, and the number of channel taps (multipath profile). Here, we assume that the length of the OFDM block is maximized without exceeding the coherence time of the channel, a selection that is in accordance with increasing the channel utilization ratio. We assume a block fading channel model where the channel is fixed during one OFDM block, but may change from one OFDM block to another. Therefore, we re-estimate the channel for every OFDM block using the dedicated pilots. The optimal ratio of pilot carriers then simply becomes a function of the average SNR and the number of channel taps.

We consider both single-element receivers and receiver arrays where maximum-ratio combining (MRC) is applied. We also consider soft detection as well as hard detection. Our results lead to a classification of channels according to their multipath profile and available SNR, where we identify regions (classes of channels) that favor either coherent or differentially coherent QPSK. The results also indicate that employing multiple receiving elements and applying soft detection have a more pronounced impact on the performance improvement of DQPSK receiver as compared to the QPSK receiver, and therefore significantly broaden the range of channels for which DQPSK outperforms QPSK.

The paper is organized as follows. In Sec. II we describe the system model. We formulate the BER and the average achievable rate in Secs. III and IV, respectively. In Sec. IV-B we extend the findings to soft decision detectors.

¹In coded systems, another way of making a fair comparison is to reduce the coding gain of coherent QPSK to below that of DQPSK, so as to leverage the pilot overhead and make the two schemes yield the same information throughput. Such an approach, however, requires selection of different coding schemes, which complicates the comparison and prevents a generalized conclusion.

Sec. V contains numerical illustration of the results. Sec. VI concludes the article.

II. SYSTEM MODEL

In a properly designed OFDM communication system with Doppler spread that is negligible with respect to carrier spacing, the signal received on the k -th carrier can be modeled as

$$y_k = H_k d_k + z_k, \quad k = 0, \dots, K - 1 \quad (1)$$

where d_k is the transmitted data symbol, H_k is the channel coefficient, and z_k is zero-mean, circularly symmetric Gaussian noise with variance σ_z^2 . We define the SNR as

$$\text{SNR} = \mathbf{E} \left\{ \frac{1}{K} \sum_{k=0}^{K-1} \frac{|H_k|^2}{\sigma_z^2} \right\} = \frac{1}{\sigma_z^2} \quad (2)$$

where we assume a normalization such that $\mathbf{E}\{|d_k|^2\} = 1$ and $\mathbf{E}\{|H_k|^2\} = 1$ for all carriers. With coherent detection, the receiver forms the QPSK decision variable as

$$\hat{d}_k = \hat{H}_k^* y_k \quad (3)$$

where \hat{H}_k is the estimated channel coefficient.

While coherent receiver estimates the channel through designated pilot carriers, differentially coherent detection relies on the assumption that the channel coefficients do not change significantly between adjacent carriers, i.e. that $H_k \approx H_{k-1}$. Here, we focus on differential encoding/detection in the frequency domain, as it simultaneously reinforces coherence across carriers and boosts the channel utilization ratio [9], [11]. The channel estimate is now effectively replaced by the signal received on the neighboring carrier.

$$\hat{b}_k = y_{k-1}^* y_k \quad (4)$$

The transmitted symbols d_k are then related to the original information symbols b_k as $d_k = b_k d_{k-1}$, with the initial symbol set to a known value, e.g. $d_0 = 1$. Note that for the coherent and differentially coherent modulations considered here, we assume that $|b_k| = |d_k| = 1$ without loss of generality.

We assume block-fading for each carrier, where the channel coefficients H_k conform to the Rayleigh model. Since all the carriers follow the same distribution, their average achievable rate will be the same. Consequently, the total average achievable rate in *bits/s/Hz* will be equal to that of one carrier. We refer to this value as the average rate.

III. BIT ERROR RATE

The achievable rate for receivers that use hard detection depends on the BER of the underlying hard detector. Therefore, we investigate the BER of the QPSK and DQPSK receivers first, and then use this BER to find the rate.

If the channel coefficients H_k obey a Rayleigh model, the average bit error rate on each carrier is given by

(see [1], Appendix C)

$$P_b = \frac{1}{2} \left(1 - \frac{\mu}{\sqrt{2 - \mu^2}} \right) \quad (5)$$

where

$$\mu = \frac{E\{y_k \hat{H}_k^*\}}{\sqrt{E\{|\hat{H}_k|^2\} E\{|\hat{y}_k|^2\}}} \quad (6)$$

is the relevant correlation coefficient. Note that μ does not depend on k as all the channel coefficients are assumed to be identically distributed.

The correlation coefficient μ depends on the receiver design, i.e. on the particular channel estimate used. Here, we compare three receivers: coherent detector with ideal channel knowledge, coherent detector with pilot-based channel estimation, and a differentially coherent detector. Since our focus is on QPSK signals, we simply refer to the coherent and differentially coherent receivers as QPSK and DQPSK in what follows.

When the channel is perfectly known to the coherent receiver, we have that $\hat{H}_k = H_k$, and the correlation coefficient becomes

$$\begin{aligned} \mu_{\text{QPSK,ideal}} &= \frac{E\{H_k(H_k + z_k)^*\}}{\sqrt{E\{|H_k|^2\} E\{|H_k + z_k|^2\}}} \\ &= \frac{1}{\sqrt{1 + \sigma_z^2}} \end{aligned} \quad (7)$$

If the channel is estimated using pilot symbols, we model the channel estimates as

$$\hat{H}_k = H_k + w_k \quad (8)$$

where w_k is the estimation error (effectively, an additional noise term) which depends on the average SNR, the number of pilots, and the particular estimation method used. An effective channel estimation algorithm exploits the sparsity of the channel impulse response. If the channel impulse response is dominated by J taps, the channel estimation error will be complex Gaussian with variance (see [12] for details)

$$\sigma_w^2 = \frac{J}{\alpha K} \sigma_z^2 \quad (9)$$

where α is fraction of the carriers designated as pilots. If the multipath delays coincide with an integer number of samples and delays are known to the receiver, then J equals the number of multipaths, P . However, if that is not the case, J will equal the multipath spread measured in samples. In general, J will be between P and the guard interval T_g measured in samples $[T_g B]$. With the channel estimation error, the correlation between the channel estimate and the received symbol will be

$$\begin{aligned} \mu_{\text{QPSK,est}} &= \frac{E\{(H_k + w_k)^*(H_k + z_k)\}}{\sqrt{E\{|H_k + w_k|^2\} E\{|H_k + z_k|^2\}}} \\ &= \frac{1}{\sqrt{(1 + \sigma_w^2)(1 + \sigma_z^2)}} \end{aligned} \quad (10)$$

TABLE 1. Calculation of the average rate for coherent and differentially coherent detectors.

Receiver	Step 1	Step 2	Step 3
QPSK, ideal ch. knowledge	set $\alpha = 0$, find μ from (7)	use μ to find BER (5)	use BER to find rate (13)
QPSK, estimated channel	choose α , find μ from (9) and (10)	use μ to find BER (5)	use BER to find rate (13)
DQPSK	set $\alpha = \frac{1}{K}$, find μ from (11)	use μ to find BER (5)	use BER to find rate (13)

Finally, with differentially coherent detection, we have

$$\begin{aligned} \mu_{DQPSK} &= \frac{E\{(H_{k-1} + z_{k-1})^*(H_k + z_k)\}}{\sqrt{E\{|H_{k-1} + z_{k-1}|^2\}E\{|H_k + z_k|^2\}}} \\ &= \frac{\lambda}{1 + \sigma_z^2} \end{aligned} \tag{11}$$

where $\lambda = E\{H_{k-1}^* H_k\}$ describes the correlation between adjacent carriers. When there is perfect coherence between adjacent carriers (very narrow carrier spacing), $\lambda = 1$, but we will also consider the case where this correlation is less than perfect.

IV. ACHIEVABLE RATE

A. HARD DETECTION

Given a communication system with QPSK modulation and an average bit error rate P_b , the ideally achievable rate is twice the capacity of the binary symmetric channels, and is given by [1]

$$\bar{R} = 2(1 + P_b \log_2 P_b + (1 - P_b) \log_2(1 - P_b)) \tag{12}$$

The rate is further decreased by the fraction α of pilots needed to estimate the channel. Therefore, the achievable rate is [13]

$$R = (1 - \alpha)\bar{R} \tag{13}$$

This rate is based on using an ideal error-correction code. Note also that we ignore the guard interval in the calculation of the achievable rate as its effect is the same for all detection methods, and we are focusing on the comparison, not absolute performance.

The BER P_b is a function of α for coherent detection, and therefore, there is a trade-off in the rate R : a small α leads to poor channel estimation, while a large α leads to high overhead. This trade-off is demonstrated in Fig. 1. Shown in the figure is the average rate as a function of the pilot ratio. Circles point to the optimal pilot ratio for which the average rate is maximized. The optimal value of α depends on the average SNR for QPSK.

It can be observed from Fig. 1 that more pilots are needed at lower SNRs. This result closely resembles the one obtained in [14], where the aim is to designate an optimal ratio of the transmit power to pilot symbols. Reference [13] also demonstrates a similar concept. For DQPSK, α is set to $1/K$, as only one symbol is sacrificed to start the differentially coherent detection.

Once the value of α is set, the correlation coefficient μ can be calculated for a given detection method, and the corresponding BER follows from (5). The BER finally determines

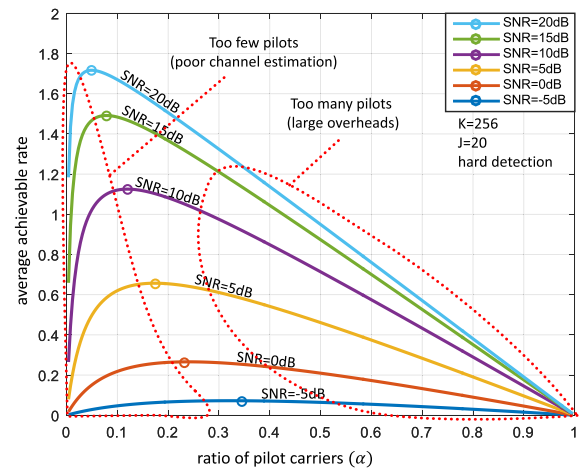


FIGURE 1. The average rate for QPSK depends on the ratio α of carriers dedicated as pilots. The OFDM blocks have 256 carriers, and the channel impulse response has 20 taps in this example.

the average rate (13). Table 1 summarizes the steps involved in calculating the average rate.

The BER performance can be significantly improved with the use of a receiver array. Given an array of M receiving elements that observe independent Rayleigh fading channels, the average BER is given by [1]

$$P_b = \frac{1}{2} \left(1 - \rho \sum_{m=0}^{M-1} \binom{2m}{m} \left(\frac{1 - \rho^2}{4} \right)^m \right) \tag{14}$$

where $\rho = \mu / \sqrt{2 - \mu^2}$, and μ can be evaluated from (7), (10) or (11) depending on the detection method. Note that since we assume independent fading across the carriers, the diversity order is the same as the number of receiver elements.

B. SOFT DETECTION

Unlike hard detection, where decisions made on the data estimates (3) are fed to the decoder, soft detection uses the estimates (3) directly. Soft detection can improve the BER performance by about 2 dB on AWGN channels [1], [15]. If differentially coherent detection is used, the same is true for the estimates (4).

For a given channel realization, the average rate of a soft detector operating with equiprobable symbols is given by the average mutual information between the transmitted and received signals (see e.g. [1, Sec. 6.4])

$$\bar{R} = \int_{\hat{d} \in \mathcal{R}^2} p_{\hat{D}|D}(\hat{d}|d) \log_2 \frac{p_{\hat{D}|D}(\hat{d}|d)}{p_{\hat{D}}(\hat{d})} d\hat{d} \tag{15}$$

where $p_{\hat{d}}(\hat{d}) = \frac{1}{4} \sum_{d_i \in \{\pm 1, \pm j\}} p_{\hat{d}|D}(\hat{d}|d_i)$ is the probability density function (pdf) of the data symbol estimate, and $p_{\hat{d}|D}(\hat{d}|d)$ is the conditional pdf, obtained for a given value of the transmitted data symbol. Without the loss of generality, we use $d = 1$ to calculate the rate. For differentially coherent detection, treatment is completely analogous, with $p_{\hat{b}}(\hat{b})$ and $p_{\hat{b}|B}(\hat{b}|b)$ replacing the pdfs pertaining to the estimate (4).

The average rate \tilde{R} given by (15) is associated with one carrier, and it corresponds to a particular channel realization H_k . The pdf $p_{\hat{d}}(\hat{d})$ is difficult to obtain in general, but its characteristic functions is readily available as a special case of the Gaussian quadratic form (see [1, Appendix B]),

$$\phi_{\hat{d}}(j\nu) = \frac{1}{2\sigma_z^2\sigma_w^2\nu^2 + 1} e^{\frac{|H_k|^2}{2\sigma_z^2\sigma_w^2\nu^2 + 1} (-\sigma_w^2 + \sigma_z^2)\nu^2 + j\nu} \quad (16)$$

The corresponding pdf can be evaluated numerically and used in (15) to calculate the rate. The same approach is used for calculating $p_{\hat{b}}(\hat{b})$; the only difference is in the values of σ_w^2 used in the characteristic function.

The rate \tilde{R} is the conditional average rate that depends on the channel, or more specifically, on the power $G = |H_k|^2$. In other words, $\tilde{R} = \tilde{R}(G)$. The average rate is obtained as

$$R = (1 - \alpha) \int_0^\infty p_G(g) \tilde{R}(g) dg \quad (17)$$

where $p_G(g)$ is the pdf of the channel strength. For Rayleigh fading, we have the exponential distribution

$$p_G(g) = e^{-g}, \quad g \geq 0 \quad (18)$$

The average rate for the three cases considered (QPSK with perfect/imperfect channel state information (CSI); DQPSK), is now obtained by replacing σ_w^2 in (16) by an appropriate value. For QPSK with perfect CSI we have that $\sigma_w^2 = 0$; for QPSK with imperfect CSI, σ_w^2 is given by (9), and for DQPSK, we have that $\sigma_w^2 = \sigma_z^2$.

V. NUMERICAL RESULTS

We present the results for on an OFDM system with 256 carriers. The corresponding symbol period is short enough to support the assumption of a block fading channel. We estimate the channel for each block using pilots if coherent detection is employed.

Fig. 2 shows the optimal pilot ratio as a function of the number of channel taps for a QPSK system. Various curves in this figure correspond to different values of the SNR and a different number of receiving elements. An interesting observation to be made from this result is that larger receiver arrays and higher SNRs require fewer pilots. This trend is explained by the fact that the achievable rate saturates at 2 bps/Hz; hence, when the SNR is high, it is beneficial to sacrifice channel estimation accuracy for reduced pilot overhead. However, the number of pilot carriers must be greater than or equal to the number of channel taps for the channel to be observable. This limit is shown in the figure as the shaded area.

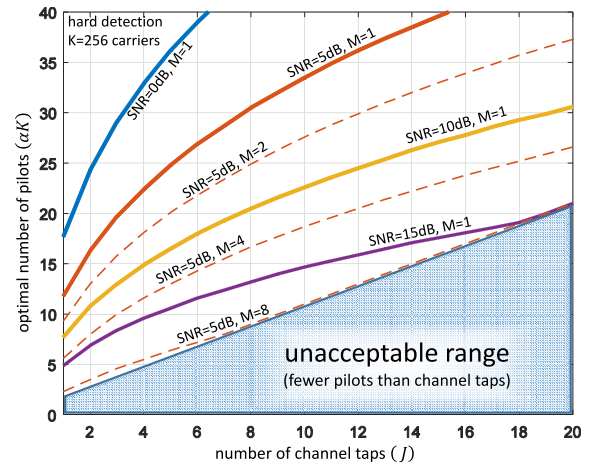


FIGURE 2. Optimal number of pilot carriers (αK) as a function of the number of channel taps that have to be estimated. Each curve corresponds to a particular SNR and the number of receiving elements M . Note that the number of pilot symbols in each OFDM block cannot be less than the number of channel taps (shaded area).

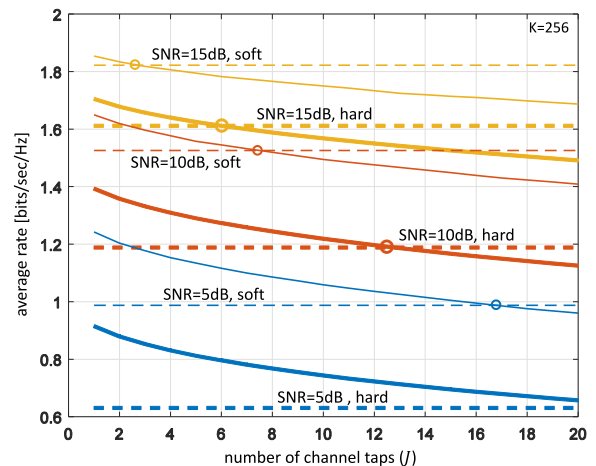


FIGURE 3. Average rate achievable by QPSK (solid) and DQPSK (dashed) vs. the number of channel taps for multiple average SNR values. If the number of channel taps is above the crossing point value (circle), QPSK cannot outperform DQPSK with any pilot carrier allocation strategy.

Throughout the rest of our analysis, we assume that the fraction of pilot carriers is selected optimally. Such selection ensures a fair comparison with differentially coherent detection which does not require pilots for channel estimation. In other words, if coherent detection is outperformed by differentially coherent detection, improper receiver design will not be the culprit.

Fig. 3 compares the average rates achievable by QPSK and DQPSK. The average rate is shown vs. the number of channel taps that need to be estimated. For QPSK, this is a decreasing function (solid curves), while DQPSK performance remains insensitive to the channel length (dashed lines). When the channel impulse response is dominated by a single tap (i.e. the frequency response is flat), QPSK outperforms DQPSK at all SNRs. However, as the number of channel taps increases,

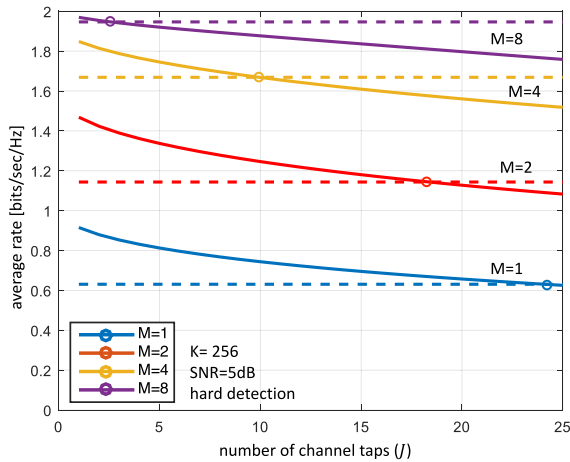


FIGURE 4. Average rate achieved by QPSK (solid) and DQPSK (dashed) vs. the number of channel taps for varying diversity order M . Fading is assumed to be uncorrelated across the receiver elements and the average SNR is 5 dB for each element.

channel estimation becomes more challenging, and the number of required pilots grows. Eventually, the cost of channel estimation reduces the average rate of QPSK to below that of DQPSK. The crossing points are marked with circles. Note that in the soft detection case, DQPSK performs better than QPSK at a lower number of channel taps than that found in the hard decision case.

Fig. 4 extends the performance comparison to multi-element receivers. As expected, diversity provides a significant improvement for both QPSK and DQPSK. As the order of diversity grows, the average rate increases, eventually saturating at the maximum of 2 bits/Hz. Note that saturation plays in favor of DQPSK as coherent detection needs at least J pilot carriers even with a high diversity order (e.g. $M = 8$).

The crossing point of the performances, indicated by circles in Figs. 3 and 4, can be interpreted as the border of a region that divides the operating conditions into those that favor coherent, and those that favor differentially coherent detection. Fig. 5 shows these regions in the multipath-SNR plane. Each delineating curve corresponds to hard/soft detection and a particular diversity order. If the channel parameters fall on the right of a delineating curve, DQPSK outperforms QPSK in terms of the average rate. Otherwise, coherent detection is the better choice, provided an optimal number of pilots. An interesting observation to be made from this figure is that as the number of receiver elements grows, the boundary moves in favor of differentially coherent detection, opening up the range of operating conditions (SNR, multipath profile) for which differentially coherent detection is the preferred choice. This effect occurs because the channel capacity saturates at 2 bits/Hz for QPSK, and therefore, at high SNR (or high diversity order) the capacity is dictated by the number of data symbols, which is greater for DQPSK.

While Fig. 5 specifies the QPSK/DQPSK preference regions, the question remains to be answered: Where do typical underwater acoustic channels fall in that figure, and

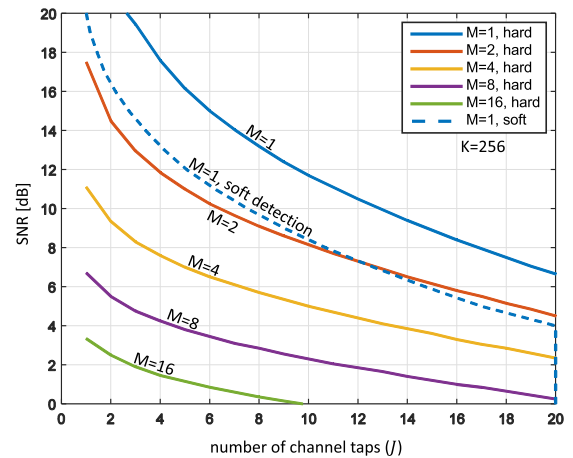


FIGURE 5. Each curve in this figure represents a summary of the crossing points (circles of Figs. 3 and 4) thus defining a delineation in the multipath-SNR plane. To the right of each delineating curve is the region in which differentially coherent detection is the preferred choice as it delivers higher average rate at lower complexity. The solid curves represent the delineation for hard detectors, while the dashed curve represents the preferred regions for soft detectors.

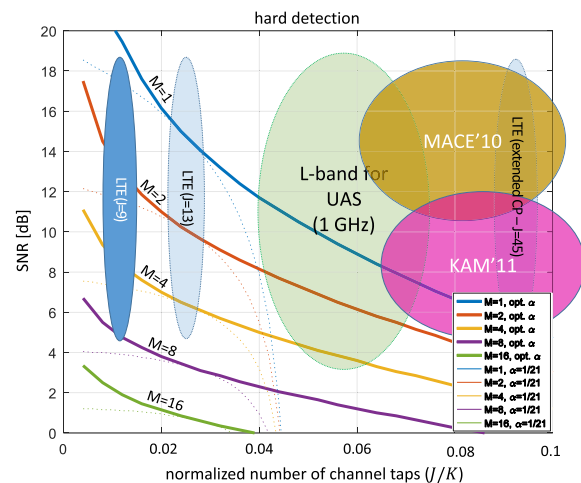


FIGURE 6. QPSK/DQPSK delineating curves for various diversity orders. Solid lines correspond to the optimally selected pilot ratio α ; dotted lines correspond to $\alpha = 1/21$, the value used in the LTE standard. Shaded ovals indicate parameters typical of several systems.

how do they compare to wireless radio channels? To answer this question, we normalize the number of channel taps to express it as a fraction of the number of carriers, and show the results in Fig. 6. Solid curves in this figure correspond to the optimally selected fraction of pilots α , while dotted curves correspond to $\alpha = 1/21$, the value used in the long-term evolution (LTE) standard. Indicated by the shaded ovals are the regions typical of several systems.

On the far right in this figure lie the channel parameters for two underwater acoustic experiments. The first experiment is the Mobile Acoustic Communications Experiment (MACE), conducted near Rhode Island in June 2010. Transmissions were made in the 10 kHz - 15 kHz acoustic band, over 2 km - 7 km in 100 m deep water. The second experiment is

the Kauai Acomms MURI (KAM) which was conducted near Kauai Island, Hawaii, in 2011. Transmissions were made in the 8 kHz - 32 kHz acoustic band over 3 km in 100 m deep water. These two experiments are labeled as MACE'10 and KAM'11 in the figure. More details about the experiments can be found in [11]. For these channels, the preferred region is clearly that of differentially coherent detection. This situation is in contrast to the typical wireless radio channels, such as those specified by the LTE standard models. We included Extended Vehicular A model (EVA), where we assumed that the receiver knows the time of arrival of all 9 paths that coincide with channel taps (i.e. $J = 9$) and the bandwidth of 2.7 MHz is occupied by 180 carriers. These channels favor coherent detection. For the same EVA channel model, if the time of path arrivals does not coincide with channel taps, and the receiver is unaware of the channel multipath intensity profile ($J = T_g B = 13$), channel estimation errors will be more pronounced, but QPSK remains the method of choice. These examples represent "extreme" radio environments, which have only recently begun to appear on the commercial stage. Ironically, these environments are also the ones that bear most resemblance to the typical acoustic environments, whose distortions have challenged system designers for decades.

While the common wireless radio channels favor coherent detection, counterexamples can be found. These cases occur with very long delay spreads or in highly time-varying environments (either due to high mobility such as with high-speed trains and aerial systems, or in systems operating at very high frequencies, e.g. 60 GHz). In Fig. 6 we have used the channel parameters measured for wireless communication with unmanned aerial systems (UAS) in the L-band frequency range (about 1 GHz) published in [16]. The result suggests that DQPSK is very competitive with QPSK and is the preferred choice at higher SNRs or when receiver arrays are employed on these channels. The main difference between the LTE standard and L-band communication for UAS is that the high speed of the UAS (i.e. up to about 860 km/h) causes significant Doppler shifts, requiring more frequent channel estimation which increases the estimation overhead.² The other example is an LTE communication system that has to operate in the extended cyclic prefix mode ($T_g = 16.7\mu s$) to accommodate longer delay spreads, and has no knowledge of the multipath intensity profile ($J = \lceil T_g B \rceil = 45$). For such a communication system, DQPSK is clearly the method of choice.

Another interesting observation to be made from Fig. 6 is the change in preference regions that occurs if the number of pilots is not selected optimally, but set to a fixed value. If we use a pre-defined pilot carrier ratio (e.g. $\alpha = 1/21$ for

²The channel impulse responses measured in [16] show at least 6 multipath arrivals ($J \geq 6$). The UAS motion at 860 km/h causes Doppler shifts as high as 800 Hz, limiting the coherence time of the channel to 250 μs . Given the 500 kHz bandwidth suggested in the L-band Digital Aeronautical Communications System (LDACS1) standard [17], the number of carriers will be limited to about 100, implying that the minimum value of J/K of about 0.06. Alternatively, if 50 carriers are used (as suggested in the LDACS1 standard), J/K will be twice as large.

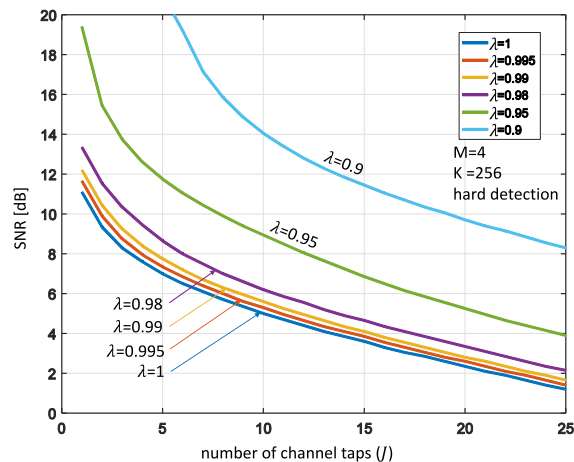


FIGURE 7. QPSK/DQPSK delineating curves for varying coherence λ between adjacent carriers.

LTE), the favorable region for DQPSK grows significantly (thin curves in Fig. 6). Note that practical systems may indeed use a pre-set number of pilots, i.e. that their achievable rate may deviate from the optimum.

Another issue to address is coherence between adjacent carriers. Referring to the expression (11), this coherence is described by the parameter λ . Fig. 7 shows the multipath-SNR delineating curves for a 4-element receiver and different values of λ . As coherence decreases from $\lambda = 1$ (full coherence, to which all previous results correspond) to values below 1, the delineating curve moves to the right, shrinking the region in which differentially coherent detection is preferred. The shrinkage, however, is not significant for practical values of λ . For example, the lowest value estimated for the MACE'10 experiment is $\lambda = 0.96$. One should also note that carrier coherence in any wireless system can be controlled by choosing the carrier spacing as narrow as the Doppler effects allow.

Finally, we investigate larger constellation sizes in Figs. 8 and 9.³ These figures depict the delineating curves for various constellation sizes. Fig. 8 includes QPSK, 8PSK and 16PSK modulations and their differentially coherent counterparts, with 1, 2 or 4 receiver elements. This figure shows that smaller constellations (i.e. QPSK and DQPSK) are optimal in a low SNR regime, but the optimal constellation size grows with SNR. Furthermore, coherent detection is outperformed by differentially coherent detection for all constellation sizes as the number of channel taps increases. As a result, each of the aforementioned constellations are the best choice in a specific set of conditions. Notably, the regions that favor differentially coherent detection expand with the number of receiver elements in a manner similar to that observed in Fig. 4.

³The derivation of the average rate for 8PSK and 16PSK are similar to QPSK and can be derived from [1, Appendix C]. For 16QAM, however, closed form relationship cannot be derived and we have used the numerical evaluation method described in [18].

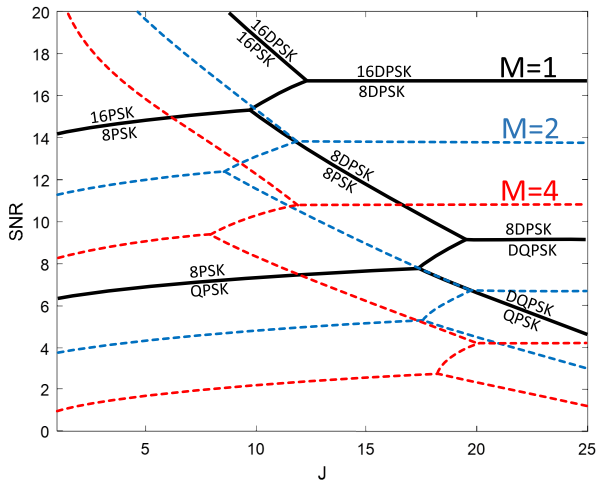


FIGURE 8. Delineating curves for QPSK, 8QPSK and 16PSK and their differential counterparts. The black, blue and red curves correspond to 1, 2 and 4 receiver elements, respectively. Note that increasing the number of receiving elements acts in favor of differentially coherent detection for all constellation sizes.

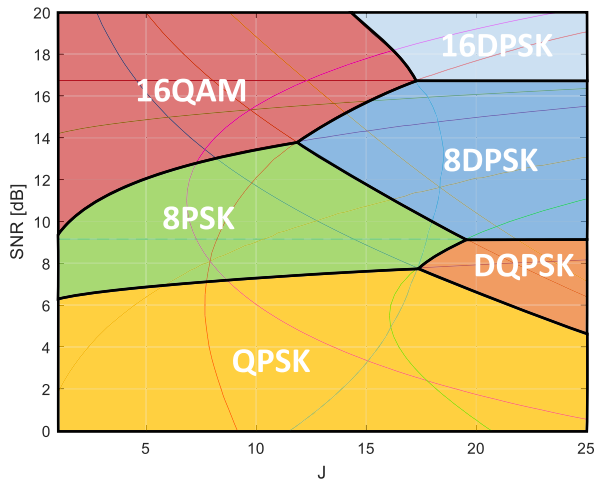


FIGURE 9. Delineating curves for QPSK, 8QPSK, 16PSK and their differential counterparts, as well as for 16QAM modulation. The optimal constellation and detection method is noted for each region. Note that 16PSK is absent because it is outperformed by other methods.

Fig. 9 includes 16QAM modulation as well as the PSK modulations of varying size. The result shows that 16PSK modulation is outperformed by 16QAM at higher SNRs, although the performance gap is minuscule. 16QAM, however, is outperformed by differential detection of 16PSK when the number of channel taps grows.

VI. CONCLUSION

We compared the average achievable rate for coherent and differentially coherent detection (QPSK and DQPSK) in OFDM systems and illustrated analytical results numerically for several practical channels. To make the comparison fair, an optimal ratio of carriers was dedicated to pilots for coherent detection. The results showed that QPSK does not necessarily outperform DQPSK. In fact, in the highly

time-varying channels with a large number of channel taps, the cost of channel estimation (pilot overhead and estimation errors) can outweigh the benefits of coherent detection. This observation is in agreement with the results obtained in [8] and [9] for certain radio channels, as well as in [11] for acoustic channels, where specific DQPSK receivers were demonstrated to be competitive or to outperform a coherent receiver.

Unlike in the existing references, where a comparison is made in terms of the BER only, our analysis was based on the achievable rate as well. We showed that the channel parameters for certain underwater acoustic channels fall in the range that favors DQPSK modulation. This observation specifically explains the experimental observations of [11], where a custom-made DQPSK receiver for underwater acoustic channels was shown to outperform a typical QPSK receiver. In contrast to the acoustic channels, QPSK can deliver higher data rates for many wireless channels including all standardized LTE channel models. This, however, does not mean that the same applies for all wireless radio channels. Counterexamples include air-ground wireless communication with unmanned aerial systems (UAS) in the L-band frequency range, and LTE communication systems operating in the extended cyclic prefix mode. On these channels, DQPSK becomes the preferred choice as it prevents an undue increase in the channel estimation overhead. Wireless channels at higher frequencies (e.g. at 60 GHz) are another good candidates for application of DQPSK. As radio systems move to higher frequency bands and greater mobility, lessons learned on acoustic channels may become useful for these systems as well.

While this paper focused on QPSK and DQPK constellations, we also showed that similar concepts apply to larger constellation sizes, and for each constellation size, the differentially coherent receiver outperforms the coherent receiver as the number of channel taps grows. Coherent 16QAM receivers were also shown to be outperformed by differentially coherent 16PSK receivers for high SNR channels with a large number of channel taps.

Finally, we showed that since channel capacity is limited by the number of data symbols at high SNR, either increasing the number of receiver elements (the diversity order), or applying soft detection has a significant effect in favor of differentially coherent detection due to its negligible pilot overhead. This is particularly important in underwater acoustic channels as array receivers are often necessary to improve the reliability of communication links.

Future work will include additional experimental analyses of underwater acoustic channels and channel models from higher frequency radio channels (e.g. 60GHz range), adding flexibility in power allocation to pilot carriers, and inclusion of higher-order constellations.

REFERENCES

[1] J. G. Proakis and M. Salehi, *Digital Communication*, 5th ed. New York, NY, USA: McGraw-Hill, 2008.

- [2] M. Stojanovic, J. G. Proakis, and J. A. Catipovic, "Analysis of the impact of channel estimation errors on the performance of a decision-feedback equalizer in fading multipath channels," *IEEE Trans. Commun.*, vol. 43, nos. 2–4, pp. 877–886, Feb. 1995.
- [3] J.-J. van de Beek, O. Edfors, M. Sandell, S. K. Wilson, and P. O. Borjesson, "On channel estimation in OFDM systems," in *Proc. IEEE 45th Veh. Technol. Conf.*, vol. 2, Jul. 1995, pp. 815–819.
- [4] Y. M. Aval, S. K. Wilson, and M. Stojanovic, "On the achievable rate of a class of acoustic channels and practical power allocation strategies for OFDM systems," *IEEE J. Ocean. Eng.*, vol. 40, no. 4, pp. 785–795, Oct. 2015.
- [5] E. Panayirci, H. Senol, and H. V. Poor, "Joint channel estimation, equalization, and data detection for OFDM systems in the presence of very high mobility," *IEEE Trans. Signal Process.*, vol. 58, no. 8, pp. 4225–4238, Aug. 2010.
- [6] H. Senol, E. Panayirci, and H. V. Poor, "Nondata-aided joint channel estimation and equalization for OFDM systems in very rapidly varying mobile channels," *IEEE Trans. Signal Process.*, vol. 60, no. 8, pp. 4236–4253, Aug. 2012.
- [7] K. S. Gomadam and S. A. Jafar, "Modulation and detection for simple receivers in rapidly time-varying channels," *IEEE Trans. Commun.*, vol. 55, no. 3, pp. 529–539, Mar. 2007.
- [8] Y. Li, L. J. Cimini, and N. R. Sollenberger, "Robust channel estimation for OFDM systems with rapid dispersive fading channels," *IEEE Trans. Commun.*, vol. 46, no. 7, pp. 902–915, Jul. 1998.
- [9] S. Lu and N. Al-Dhahir, "Coherent and differential ICI cancellation for mobile OFDM with application to DVB-H," *IEEE Trans. Wireless Commun.*, vol. 7, no. 11, pp. 4110–4116, Nov. 2008.
- [10] M. Chowdhury, A. Manolakos, and A. J. Goldsmith, "Coherent versus noncoherent massive SIMO systems: Which has better performance?" in *Proc. IEEE Int. Conf. Commun. (ICC)*, Jun. 2015, pp. 1691–1696.
- [11] Y. M. Aval and M. Stojanovic, "Differentially coherent multichannel detection of acoustic OFDM signals," *IEEE J. Ocean. Eng.*, vol. 40, no. 2, pp. 251–268, Apr. 2015.
- [12] M. Morelli and U. Mengali, "A comparison of pilot-aided channel estimation methods for OFDM systems," *IEEE Trans. Signal Process.*, vol. 49, no. 12, pp. 3065–3073, Dec. 2001.
- [13] N. Jindal and A. Lozano, "A unified treatment of optimum pilot overhead in multipath fading channels," *IEEE Trans. Commun.*, vol. 58, no. 10, pp. 2939–2948, Oct. 2010.
- [14] X. Cai and G. B. Giannakis, "Error probability minimizing pilots for OFDM with M-PSK modulation over Rayleigh-fading channels," *IEEE Trans. Veh. Technol.*, vol. 53, no. 1, pp. 146–155, Jan. 2004.
- [15] G. Ungerboeck, "Channel coding with multilevel/phase signals," *IEEE Trans. Inf. Theory*, vol. 28, no. 1, pp. 55–67, Jan. 1982.
- [16] D. W. Matolak, "Unmanned aerial vehicles: Communications challenges and future aerial networking," in *Proc. Int. Conf. Comput., Netw. Commun. (ICNC)*, Feb. 2015, pp. 567–572.
- [17] M. Schnell, U. Epple, D. Shutin, and N. Schneckenburger, "LDACS: Future aeronautical communications for air-traffic management," *IEEE Commun. Mag.*, vol. 52, no. 5, pp. 104–110, May 2014.
- [18] X. Tang, M. S. Alouini, and A. J. Goldsmith, "Effect of channel estimation error on M-QAM BER performance in Rayleigh fading," *IEEE Trans. Commun.*, vol. 47, no. 12, pp. 1856–1864, Dec. 1999.



and underwater acoustic networks.

YASHAR M. AVAL received the degree from the University of Tehran, Tehran, Iran, in 2002, the M.S. degree in electrical engineering from the Sharif University of Technology, Tehran, in 2005, and the Ph.D. degree in electrical engineering from Northeastern University, Boston, MA, USA, in 2015. He is currently an Associate Research Engineer with Northeastern University. His research interests include digital communication, OFDM, underwater acoustic communication,



SARAH KATE WILSON received the A.B. degree in mathematics from Bryn Mawr College and the Ph.D. degree in electrical engineering from Stanford University.

She has experience in both academia and industry. She is currently an Electrical Engineer specializing in digital communications. She is also a Professor of electrical engineering with Santa Clara University. Her research area includes wireless radio frequency communications, visible-light communications, and underwater acoustic communications.

Dr. Wilson received the IEEE Communications Society Joseph LoCicero Award for Exemplary Service to Publications. She was the IEEE Communications Society Director of Journals for the term 2012–2013, overseeing four society journals and their editors-in-chief. She was an Elected Vice President for Publications for the IEEE Communications Society for the term 2014–2015, overseeing all journals, magazines, and online content. Recently, she was a Co-General Chair (with Andrea Goldsmith) of the IEEE Wireless Communications and Networking Conference in San Francisco in 2017. She served as the Editor-in-Chief for the IEEE COMMUNICATIONS LETTERS from 2009 to 2011. She has been an Associate Editor of the IEEE TRANSACTIONS ON WIRELESS COMMUNICATIONS, the IEEE COMMUNICATIONS LETTERS, the IEEE TRANSACTIONS ON COMMUNICATIONS, and the *Journal of Communications and Networks*.



MILICA STOJANOVIC (SM'08–F'10) received the degree from the University of Belgrade, Serbia, in 1988, and the M.S. and Ph.D. degrees in electrical engineering from Northeastern University, Boston, MA, USA, in 1991 and 1993, respectively. She was a Principal Scientist with the Massachusetts Institute of Technology. In 2008, she joined Northeastern University, where she is currently a Professor of electrical and computer engineering. She is also a Guest Investigator with the Woods Hole Oceanographic Institution and a Visiting Scientist with MIT. Her research interests include digital communications theory, statistical signal processing and wireless networks, and their applications to underwater acoustic systems. She is the Chair of the IEEE Ocean Engineering Society's Technical Committee for Underwater Communication, Navigation and Positioning. She was an Associate Editor of the IEEE TRANSACTIONS ON SIGNAL PROCESSING and the IEEE TRANSACTIONS ON VEHICULAR TECHNOLOGY. She is an Associate Editor of the IEEE JOURNAL OF OCEANIC ENGINEERING. She also serves on the Advisory Board of the IEEE COMMUNICATION LETTERS.

...